



**HAL**  
open science

## Optimized Methods for the Surface Immobilization of Collagens and Collagen Binding Assays

Nadia Chaher, Giuseppe Digilio, Sara Lacerda, René Botnar, Alkystis  
Phinikaridou

► **To cite this version:**

Nadia Chaher, Giuseppe Digilio, Sara Lacerda, René Botnar, Alkystis Phinikaridou. Optimized Methods for the Surface Immobilization of Collagens and Collagen Binding Assays. Journal of visualized experiments: JoVE, 2023, 193, 10.3791/64720 . hal-04124237

**HAL Id: hal-04124237**

**<https://hal.science/hal-04124237v1>**

Submitted on 24 Oct 2023

**HAL** is a multi-disciplinary open access archive for the deposit and dissemination of scientific research documents, whether they are published or not. The documents may come from teaching and research institutions in France or abroad, or from public or private research centers.

L'archive ouverte pluridisciplinaire **HAL**, est destinée au dépôt et à la diffusion de documents scientifiques de niveau recherche, publiés ou non, émanant des établissements d'enseignement et de recherche français ou étrangers, des laboratoires publics ou privés.

1 **TITLE:**

2 Optimized Methods for the Surface Immobilization of Collagens and Collagen Binding Assays

3

4 **AUTHORS AND AFFILIATIONS:**

5 Nadia Chaher<sup>1</sup>, Giuseppe Digilio<sup>2\*</sup>, Sara Lacerda<sup>3\*</sup>, René M Botnar<sup>1,4,5,6</sup>, Alkystis  
6 Phinikaridou<sup>1,4+</sup>

7

8 <sup>1</sup>School of Biomedical Engineering and Imaging Sciences, King's College London, St Thomas'  
9 Hospital, London, UK

10 <sup>2</sup>Dipartimento di Scienze e Innovazione Tecnologica, Università del Piemonte Orientale,  
11 Vercelli, Italy

12 <sup>3</sup>Centre de Biophysique Moléculaire, CNRS UPR 4301, Université d'Orléans, Orléans, France

13 <sup>4</sup>BHF Centre of Research Excellence, Cardiovascular Division, King's College London, London,  
14 UK

15 <sup>5</sup>Escuela de Ingeniería, Pontificia Universidad Católica de Chile, Santiago, Chile

16 <sup>6</sup>Instituto de Ingeniería Biológica y Médica, Pontificia Universidad Católica de Chile,  
17 Santiago, Chile

18

19 \*These authors contributed equally.

20

21 Email addresses of the co-authors:

22 Nadia Chaher (nadia.chaher@kcl.ac.uk)

23 Giuseppe Digilio (giuseppe.digilio@uniupo.it)

24 Sara Lacerda (sara.lacerda@cnrs.fr)

25 René M Botnar (rene.botnar@kcl.ac.uk)

26

27 <sup>+</sup>Corresponding author:

28 Alkystis Phinikaridou (alkystis.1.phinikaridou@kcl.ac.uk)

29

30 **SUMMARY:**

31 This work presents an optimized protocol to reproducibly immobilize and quantify type I  
32 and III collagen onto microplates, followed by an improved *in vitro* binding assay protocol to  
33 study collagen–compound interactions using a time-resolved fluorescence method. The  
34 subsequent step-by-step data analysis and data interpretation are provided.

35

36 **ABSTRACT:**

37 Fibrosis occurs in various tissues as a reparative response to injury or damage. If excessive,  
38 however, fibrosis can lead to tissue scarring and organ failure, which is associated with high  
39 morbidity and mortality. Collagen is a key driver of fibrosis, with type I and type III collagen  
40 being the primary types involved in many fibrotic diseases. Unlike conventional protocols  
41 used to immobilize other proteins (e.g., elastin, albumin, fibronectin, etc.), comprehensive  
42 protocols to reproducibly immobilize different types of collagens to produce stable coatings  
43 are not readily available. Immobilizing collagen is surprisingly challenging because multiple  
44 experimental conditions may affect the efficiency of immobilization, including the type of  
45 collagen, the pH, the temperature, and the type of microplate used. Here, a detailed  
46 protocol to reproducibly immobilize and quantify type I and III collagens to create stable and  
47 reproducible gels/films is provided. Furthermore, this work demonstrates how to perform,

48 analyze, and interpret *in vitro* time-resolved fluorescence binding studies to investigate the  
49 interactions between collagens and candidate collagen-binding compounds (e.g., a peptide  
50 conjugated to a metal chelate carrying, for example, europium [Eu(III)]). Such an approach  
51 can be universally applied to various biomedical applications, such as in the field of  
52 molecular imaging to develop targeted imaging probes, drug development, cell toxicity  
53 studies, cell proliferation studies, and immunoassays.

54

#### 55 **INTRODUCTION:**

56 The accumulation of fibrous connective tissue as part of the natural wound-healing process  
57 following tissue injury is known as fibrosis. However, if the deposition of fibrous tissue fails  
58 to terminate and continues beyond what is needed for tissue repair, then fibrosis becomes  
59 excessive<sup>1,2</sup>. Excessive fibrosis impairs organ physiology and function and could lead to  
60 organ damage and potentially organ failure<sup>3-5</sup>. Two main drivers of fibrosis are the  
61 extracellular matrix (ECM) proteins collagen type I and type III<sup>6</sup>. Collagen is a structural  
62 protein found in various organs that makes up approximately one-third of the total protein  
63 content of the human body<sup>1</sup>. There are 28 different types of collagens identified by human  
64 genome sequencing, and the most abundant are the fibrillar collagens<sup>7</sup>. The primary  
65 fibrillary collagen is type I collagen, which provides the ECM with tensile strength and  
66 resistance to deformation<sup>8</sup>. Type III collagen is a structural component that provides  
67 elasticity and colocalizes with type I collagen. It is expressed during embryogenesis and is  
68 naturally found in small amounts in adult skin, muscle, and blood vessels<sup>9</sup>.

69

70 *In vivo* collagen synthesis begins with an intracellular process in which mRNA is transcribed  
71 in the nucleus and then moves to the cytoplasm, where it is translated. After translation, the  
72 chain formed undergoes post-translational modification in the endoplasmic reticulum,  
73 where pro-collagen (the precursor of collagen) is formed. The pro-collagen then travels to  
74 the Golgi apparatus for final modification before being excreted to the extracellular space<sup>10</sup>.  
75 Through proteolytic cleavage, the procollagen is transformed into tropocollagen. This is then  
76 cross-linked either *via* an enzymatic-mediated cross-linking pathway catalyzed by the  
77 enzyme lysyl oxidase (LOX) or *via* a non-enzymatic-mediated cross-linking pathway involving  
78 the Maillard reaction<sup>11</sup>. However, *in vitro* protocols to immobilize collagen mainly rely on  
79 the ability of collagen to self-assemble. Collagen is extracted from tissues based on its  
80 solubility, which largely depends on the extent of cross-linking of individual collagen fibrils<sup>7</sup>.  
81 Fibrillar collagen is dissolved in acetic acid, and fibrils can reform when the pH and  
82 temperature are adjusted<sup>12</sup>. *In vitro*, the fibrillogenesis of collagen can be viewed as a two-  
83 stage process<sup>7</sup>. The first stage is the nucleation phase, where collagen fibers form dimers  
84 and trimer fibrils before they are rearranged to form a triple helical structure. The second  
85 phase is the growth phase, whereby the fibrils start to grow laterally and result in the  
86 characteristic D-band formation, which is generally observed by changes in turbidity<sup>7</sup>.  
87 Atomic force microscopy (AFM) studies have also revealed that type I and type III collagen  
88 have different characteristics (Erreur ! Source du renvoi introuvable.)<sup>13</sup>.

89

90 To study the binding interactions between collagen and other compounds, collagen needs  
91 to be reproducibly immobilized into the wells of microplates. There are various protocols for  
92 immobilizing soluble collagen<sup>14-16</sup>. Commercially available microplates that are pre-coated  
93 with collagen are typically used for cell culture. However, pre-coated microplates have a  
94 very thin layer of an unknown amount of collagen coated onto the wells, which makes them

95 unsuitable for *in vitro* binding assays. There are several challenges when immobilizing  
96 collagen onto the plate wells. One of the key challenges is choosing a suitable type of  
97 microplate, because different types of collagens (e.g., type I and III) have different chemical  
98 properties and, therefore, immobilize more stably and effectively depending on the material  
99 of the microplate. Another challenge is the experimental conditions of the immobilization  
100 protocol, as the process of fibrillogenesis depends on multiple factors, including  
101 temperature, pH, the stock concentration of collagen, and the ionic concentration of the  
102 buffer<sup>7</sup>.

103

104 For studying the interactions between the collagen (the target) and other compounds (i.e., a  
105 targeting peptide), it is also necessary to develop a robust screening assay to investigate the  
106 specificity and selectivity of the compound toward the target by measuring the dissociation  
107 constant,  $K_d$ . The position of the equilibrium of formation of a bimolecular complex between  
108 a protein (collagen) and a ligand is expressed in terms of the association constant  $K_a$ , whose  
109 magnitude is proportional to the binding affinity. However, most commonly, biochemists  
110 express affinity relationships in terms of the equilibrium dissociation constant,  $K_d$ , of the  
111 binary complex, which is defined as  $K_d = 1/K_a \cdot K_d$  and is the inverse of  $K_a$ ; the lower the  $K_d$   
112 value, the stronger the binding strength between the protein and the ligand. The advantage  
113 of using  $K_d$  to compare the binding affinity of different ligands for the same protein (and the  
114 other way around) is linked to the fact that the units of  $K_d$  for a bimolecular complex are  
115 mol/L (i.e., concentration units). Under most experimental conditions, the  $K_d$  value  
116 corresponds to the ligand concentration that leads to 50% saturation of the available  
117 binding sites on the target at the equilibrium<sup>17,18</sup>. The dissociation constant is typically  
118 extracted by analyzing the receptor fractional occupancy (FO), which is defined as the ratio  
119 between the occupied binding sites and total available binding sites, as a function of ligand  
120 concentration. This can be done provided that an analytical assay able to distinguish and  
121 measure the amount of bound ligand is available.

122

123 *In vitro* ligand binding assays can be performed using various bioanalytical methods,  
124 including optical photometry, radioligand methods, inductively coupled plasma mass  
125 spectrometry (ICP-MS), and surface plasmon resonance (SPR). Amongst the photometric  
126 methods, those based on fluorescence emission typically require the labeling of ligands or  
127 proteins with fluorophores to increase the sensitivity and to improve the detection limit of  
128 the assay. Chelates of certain lanthanides(III) ions, such as Eu(III), are very attractive as  
129 fluorophores as they have large Stokes' shifts, narrow emission bands (providing a good  
130 signal-to-noise ratio), limited photobleaching, and long emission lifetimes. Importantly, the  
131 latter property enables the use of time-resolved fluorescence (TRF) from Eu(III) fluorophores  
132 to abolish background autofluorescence<sup>19</sup>. In the dissociation-enhanced lanthanide  
133 fluorescent immunoassay (DELFI) version of the Eu(III)-based TRF assay, ligands labeled  
134 with a non-luminescent Eu(III)-chelate are incubated with the receptor immobilized onto  
135 microplates. The labeled ligand/receptor complex is separated from the unbound ligand,  
136 and Eu(III) fluorescence is activated by dissociation of the Eu(III) complex at an acidic pH,  
137 followed by re-complexation with a fluorescence-enhancing chelator to form a micelle-  
138 embedded, highly fluorescent Eu(III) complex<sup>20</sup>.

139

140 The decomplexation step can be reasonably achieved with chelators, such as  
141 diethylenetriamine pentaacetate (DTPA), that show fast decomplexation kinetics. However,

142 Eu(III) complexes with certain macrocyclic chelators, such as DOTA (1,4,7,10-  
143 tetraazacyclododecane-1,4,7,10-tetraacetic acid) and its monoamide derivatives (DO3AAm),  
144 show high thermodynamic stability and very high kinetic inertness. In this case, the  
145 decomplexation steps must be accurately optimized to achieve sufficient and reproducible  
146 activation of Eu(III)-based TRF<sup>21</sup>. It is worth noting that lanthanide (Ln(III))-DOTA and Ln(III)-  
147 DO3AAm complexes are those most commonly employed as contrast agents for *in vivo*  
148 molecular imaging by magnetic resonance imaging (MRI) techniques<sup>22</sup>. Thus, the Ln(III)-  
149 based TRF assay is the tool of choice to study *in vitro* the binding affinity of MRI molecular  
150 probes with their intended biological targets. Currently, comprehensive and reproducible  
151 protocols for immobilizing type I and type III collagen and a reproducible pipeline for  
152 performing *in vitro* binding Eu(III) TRF experiments are lacking. To overcome these  
153 limitations, reproducible methods to self-assemble and immobilize type I and type III  
154 collagen and generate stable gels and films, respectively, with the sufficient concentration  
155 of collagen required for *in vitro* binding assays, were developed. An optimized protocol for  
156 Eu(III) TRF of highly inert Eu(III)-DO3AAm-based complexes is presented. Finally, an  
157 optimized *in vitro* microplate Eu(III) TRF assay to measure the  $K_d$  of Eu(III)-labeled ligands  
158 toward immobilized type I and type III collagen is demonstrated (**Figure 1**).

159

#### 160 **PROTOCOL:**

161 NOTE: All product information used for this work is presented in the **Table of Materials**.

162

#### 163 **1. Collagen immobilization**

164

165 NOTE: Ensure each well in the microplate used during the binding assay has adjacent wells  
166 free to avoid cross-fluorescence. Carry out this part of the protocol on ice because collagen  
167 self-assembles at rising temperatures and pH levels. Perform this procedure in a tissue  
168 culture hood and under sterile conditions because the microplates are subsequently  
169 incubated in a tissue culture (TC) incubator.

170

171 1.1. Immobilization of type I collagen on the 96-well microplates (**Figure 2: Workflow to**  
172 **immobilize type I collagen**)

173

#### 174 **Day 1**

175

176 1.1.1. Prepare a silicone tray with ice. Place the vial containing type I collagen, the cold 10x  
177 phosphate-buffered saline (PBS), and the microplates on ice, and spray everything with 70%  
178 ethanol. Place the material under the TC hood.

179

180 1.1.2. Neutralize the collagen using equal volumes of type I collagen and 10x PBS (pH 7.4).

181

182 1.1.3. Invert the solution a few times, ensuring that no bubbles form.

183

184 1.1.4. Add 100  $\mu$ L of the neutralized collagen to every other well of the microplate, and  
185 incubate at 37 °C for 18–20 h to evaporate the collagen to dryness.

186

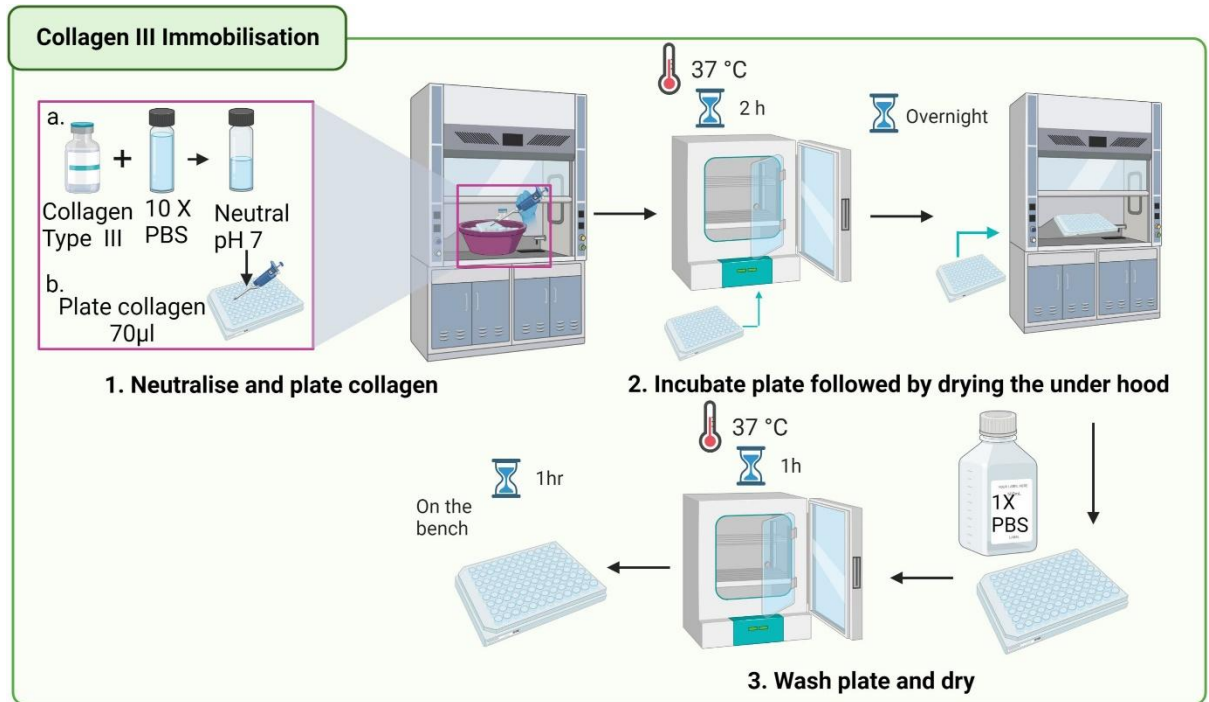
#### 187 **Day 2**

188

189 1.1.5. Wash the microplates with 100  $\mu$ L of 1x PBS, pH 7.4, twice to remove any unbound  
190 collagen.

191  
192 1.1.6. Transfer the microplates into the incubator at 37° C for another 2 h to dry before  
193 using them for further binding experiments.

194  
195 1.2. Immobilization of collagen type III on the 96-well microplates (



196 1.3.

197 1.4. **Figure 3)**

198

199 **Day 1**

200

201 1.2.1. Prepare a silicone tray with ice. Place the vial containing type III collagen, the cold  
202 10x PBS, and the microplates on ice, and spray everything with 70% ethanol. Place the  
203 material under the TC hood.

204

205 1.2.2. Neutralize the collagen using equal volumes of type III collagen and 10x PBS (pH 7.4).

206

207 1.2.3. Add 70  $\mu$ L of the neutralized collagen to every other well of the microplate, and  
208 incubate at 37 °C for 2 h by placing the microplate under the tissue culture hood to  
209 evaporate the collagen to dryness.

210

211 **Day 2**

212

213 1.2.4. Wash the microplates with 70  $\mu$ L of 1x PBS, pH 7.4, twice to remove any unbound  
214 collagen.

215

216 1.2.5. Transfer the microplates to the incubator for 1 h at 37 °C, and then transfer the  
217 microplates to the bench, and allow them 1 h to dry before using them in further binding  
218 experiments.

219

## 220 **2. Assessment of the stability of the immobilized collagen gels/films**

221

### 222 2.1. Incubation with PBS for 1 h

223

224 NOTE: During the binding experiment, incubate the immobilized collagen with the  
225 compound of interest. It is important to investigate the stability of the resulting collagen gel  
226 or film. To do this, measure the stability of three conditions: **no wash** = measures the  
227 immobilized collagen directly after incubation; **washing** = measures the immobilized  
228 collagen after washing the plate twice with 100  $\mu\text{L}$  of PBS; and **1 h PBS mimic & wash** =  
229 measures the immobilized collagen after incubating for 1 h with PBS followed by two  
230 rounds of washes with PBS. Below, the PBS incubation method is explained.

231

232 2.1.1. Add 70  $\mu\text{L}$  of PBS (1x) to each of the wells coated with collagen, and incubate the  
233 microplate at room temperature for 1 h.

234

235 2.1.2. Aspirate the excess liquid from each well using a pipette, and wash with PBS (1x)  
236 twice before carrying out the protein quantification assay described below.

237

### 238 2.2. Quantification of the amount of immobilized collagen using a bicinchoninic acid 239 assay (BCA)

240

241 NOTE: Use the Pierce BCA Protein Assay Kit (**Table of Materials**) following the  
242 manufacturer's instructions. Make respective collagen standards for this assay. The  
243 concentration range for collagen I is from 0–3,000  $\mu\text{g}/\text{mL}$  and for collagen III from 0–750  
244  $\mu\text{g}/\text{mL}$ . In total, make 11 standards per collagen.

245

246 2.2.1. Prepare the total volume of working reagent (WR) needed by following the  
247 manufacturer's instructions.

248

249 2.2.2. Add 25  $\mu\text{L}$  of each of the collagen standard into the microplate wells (in duplicate).  
250 These solutions are used to draw the standard curve.

251

252 2.2.3. Add 200  $\mu\text{L}$  of working reagent solution to each of the wells containing the standards  
253 and the wells coated with unknown concentrations of collagen.

254

255 2.2.4. Place the microplate on a plate shaker for 30 s. Cover the microplates, and incubate  
256 at 37  $^{\circ}\text{C}$  for 30 min.

257

258 2.2.5. Remove the microplates, and allow to cool at room temperature. Measure the  
259 absorbance at 560 nm using a plate reader.

260

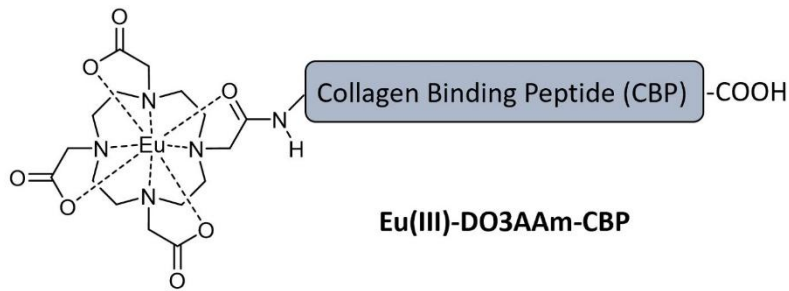
261 2.2.6. Plot a calibration curve by plotting the  $A_{560}$  (AU) versus the concentration ( $\mu\text{g}/\text{mL}$ ) of  
262 the 11 standard solutions, and use the calibration curve to calculate the amount of collagen.

263

## 264 **3. Europium(III) TRF ligand binding assay (Figure 1)**

265

266 NOTE: The compound used is a candidate collagen-binding peptide (CBP) labeled with a  
267 single Eu(III)-DO3AAm complex, referred to as Eu(III)-DO3AAm-CBP (



268  
269 **Figure 4).**

270  
271 3.1. Incubation of the collagen-coated plates with the Eu(III)-DO3AAm-CBP compound

272

273 3.1.1. Prepare solutions of the Eu(III)-DO3AAm-CBP compound with concentrations ranging  
274 between 0.1–15  $\mu\text{M}$  (0.1  $\mu\text{M}$ , 0.5  $\mu\text{M}$ , 1  $\mu\text{M}$ , 3  $\mu\text{M}$ , 5  $\mu\text{M}$ , 7  $\mu\text{M}$ , 10  $\mu\text{M}$ , and 15  $\mu\text{M}$ ) in 1x  
275 PBS.

276

277 3.1.2. Add 75  $\mu\text{L}$  of each concentration of compound into the collagen-coated wells (Plate  
278 A). Perform the experiment in triplicate to calculate the amount of compound that binds to  
279 the collagen.

280

281 3.1.3. Use a second uncoated plate (Plate B), and add 75  $\mu\text{L}$  of each compound to the  
282 empty wells to calculate the non-specific binding of the compound to the plate. Use  
283 triplicates for each concentration.

284

285 3.1.4. Incubate the microplates for 1 h at room temperature.

286

287 3.1.5. Using a pipette, aspirate and discard the excess solution from each well, and wash  
288 the wells with 1x PBS twice to remove excess, unbound compound. Perform this step using  
289 both the collagen-coated and uncoated microplates.

290

291 3.1.6. To a third uncoated plate (Plate C), add 10  $\mu\text{L}$  of the same range of Eu(III)-DO3AAm-  
292 CBP concentrations (in duplicate). Use the fluorescence reading from the Eu(III)-DO3AAm-  
293 CBP in solution to make a calibration curve.

294

295 NOTE: Do not wash or aspirate the solution from this plate.

296

297 3.2. Acid extraction of Europium(III) and time-resolved fluorescence (TRF) readings

298

299 NOTE: Please refer to the supplemental information about the preparation and calibration  
300 of the volumes of the acidic solution (AS) and the buffering solution (BS). The volumes of the  
301 AS and BS required to reproducibly achieve an optimal pH were 54  $\mu\text{L}$  and 46  $\mu\text{L}$ ,  
302 respectively, in this work. Carry out the following operation on plate A, plate B, and plate C.

303



304 3.2.1. Add 54  $\mu\text{L}$  of acidic solution (AS) to each well, and place the plate in the incubator at  
305 37  $^{\circ}\text{C}$  for 90 min, covering the microplates with foil to avoid evaporation. The temperature  
306 and incubation time must be carefully controlled to achieve reproducible decomplexation.

307

308 3.2.2. Add 46  $\mu\text{L}$  of buffering solution (BS) to each well, and gently shake the plate for 30 s.

309

310 3.2.3. Add 100  $\mu\text{L}$  of enhancement solution (ES), and shake the plate for 30 s.

311

312 3.2.4. Wait for 30 min before reading the plate using a TRF plate reader. Use the  
313 parameters listed in Erreur ! Source du renvoi introuvable..

314

#### 315 **4. Data analysis**

316

317 4.1. Quantification of the concentration of collagen immobilized on the wells

318

319 4.1.1. Obtain the equation of the calibration curve of the  $A_{560}$  (AU) versus the  
320 concentration ( $\mu\text{g}/\text{mL}$ ) of the 11 standard solutions.

321

322 4.1.1.1. Use the absorbance readings acquired from the wells containing the collagen  
323 standards.

324

325 4.1.1.2. Tabulate the average values from the duplicate wells, and plot the mean  
326 absorbance against the known protein (collagen) concentrations ( $\mu\text{g}/\text{mL}$ ) to obtain the  
327 equation for the standard curve.

328

329 4.1.2. Use the absorbance values to calculate the mass ( $\mu\text{g}$ ) and concentration (M) of  
330 immobilized collagen.

331

332 4.1.2.1. Compute the average absorbance values across the three wells that  
333 contained immobilized collagen, and record the standard deviation.

334

335 4.1.2.2. Use the standard curve equation obtained from the collagen standard curve  
336 (step 2.2.6) to convert the absorbance measured from the collagen-coated wells into  
337 concentration. From this, calculate the concentration of collagen that was immobilized within  
338 the experimental wells in  $\mu\text{g}/\text{mL}$ .

339

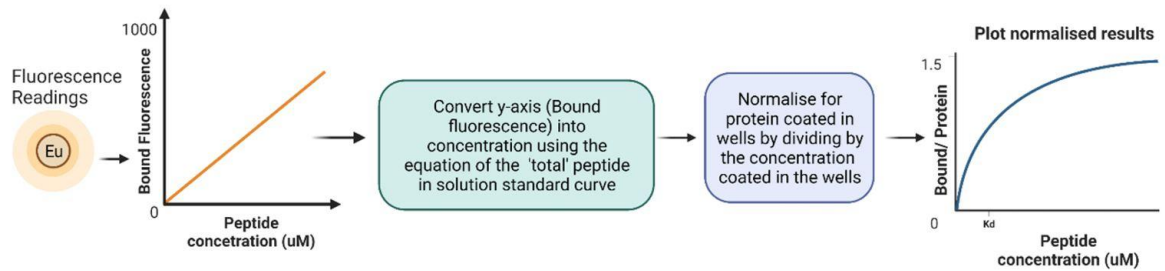
340 4.1.2.3. Convert the concentration calculated in step 4.1.2.2 ( $\mu\text{g}/\text{mL}$ ) first to  
341 grams/liter and, based on the molecular weight of the collagen, into molar (M).

342

343 4.1.2.4. Finally, calculate the mass of the collagen immobilized in each well by  
344 dividing the concentration by the volume of collagen added to the well (100  $\mu\text{L}$  for type I  
345 collagen and 70  $\mu\text{L}$  for type III collagen).

346

347 4.2. Calculation of the dissociation constant ( $K_d$ ) (



348 4.3.  
 349 4.4. **Figure 5)**

350  
 351 4.4.1. Extract the fluorescence readings.  
 352

353 4.4.1.1. Export the fluorescence readings from the plate reader to a spreadsheet.  
 354

355 NOTE: In binding assays, it is important to account for the potential non-specific binding of a  
 356 compound to the plastic surface of the plates  
 357

358 4.4.1.2. Calculate the mean values of triplicate measurements from each compound  
 359 concentration for the three different plates: the specific binding readings from the coated  
 360 wells (Plate A), the non-specific binding from the uncoated wells (Plate B) and the total  
 361 Eu(III)-DO3AAM-CBP in solution in the uncoated wells (Plate C).  
 362

363 4.4.1.3. Determine the fluorescence values for the bound compound by subtracting  
 364 the fluorescence readings of the uncoated wells (Plate B) from that of the coated wells  
 365 (Plate A).  
 366

367 Equation 1: Determining the bound fluorescence<sup>17</sup>:

$$\text{Bound fluorescence} = \text{Specific (coated wells)} - \text{Unspecific (uncoated well)}$$

368  
 369 4.4.1.4. Generate a calibration curve using the readings from the Eu(III)-labeled  
 370 compound in solution (Plate C). Plot the fluorescence readings obtained against the  
 371 concentration of the Eu(III)-labeled compound. Perform a linear regression fit.  
 372

373 4.4.2. Convert the fluorescence readings to concentrations.  
 374

375 4.4.2.1. Convert the readings of the bound fluorescence (step 4.2.3) into  
 376 concentration using the standard fluorescence curve from the data generated using the  
 377 compound concentrations in solution (step 4.2.1.4).  
 378

379 NOTE: When comparing the binding properties of one compound toward different target  
 380 proteins that immobilize at different concentrations, the latter will need to be considered  
 381 when calculating the amount of compound bound to the target (i.e., bound  
 382 compound/protein).  
 383

384 4.4.2.2. Divide the concentration of the bound compound by the concentration of the  
 385 protein immobilized in the well.  
 386

387 NOTE: For this calculation, use the concentration of immobilized collagen that was  
388 calculated after the wells were incubated with PBS for 1 h (so-called PBS mimic experiment;  
389 section 2.1 above). This is to account for potential losses of collagen during the incubation  
390 step and washing step so that those losses will not contribute to the final fluorescence  
391 signal.

392

393 4.4.2.3. Plot the data using a scatter plot that has the concentrations of the  
394 compound on the x-axis ( $\mu\text{M}$ ) and the bound compound/protein on the y-axis.

395

396 4.4.3. Obtain the  $K_d$  values.

397

398 4.4.3.1. Fit the data acquired in step 4.2.2.3 using two possible binding kinetic  
399 models: one-site binding and one-site binding with a hill slope. The equations for each  
400 model are shown in Erreur ! Source du renvoi introuvable..

401

402 4.4.3.2. Choose the model that provides a non-ambiguous fitting with the highest R-  
403 squared value when fitting the data.

404

405 4.4.3.3. Exclude the outliers (s) for each set of fluorescence readings per  
406 concentration per plate.

407

408 4.4.3.4. Calculate the final  $K_d$  value, and present the data as the mean  $\pm$  standard  
409 deviation of independent experiments.

410

411 NOTE: For robust results, perform triplicate measurements within each plate and at least  
412 three independent experiments with different microplates.

413

414 4.4.4. Calculate the fractional occupancy (FO).

415

416 NOTE: From Equation 2, the concentration of the target is unknown, and, therefore, by  
417 using algebra and the  $K_d$ , from Equation 3, a workable equation for calculating the fractional  
418 occupancy arises in the form of Equation 4.

419

420 Equation 2: Definition of fractional occupancy<sup>17</sup>:

421

$$\text{Fractional Occupancy} = \frac{()}{(\text{target}) + (\text{compound} \cdot \text{target})}$$

422

423

424 Equation 3: The dissociation constant,  $K_d$ , which is the concentration at which the  
425 compound occupies 50% of the target at equilibrium<sup>17</sup>:

426

$$\frac{(\text{compound}) \cdot (\text{target})}{\text{compound} \cdot \text{target}} = \frac{K_{off}}{K_{on}} = K_d$$

427

428 Equation 4: Rearranged equation to calculate the FO equation<sup>17</sup>:

$$\text{Fractional Occupancy} = \frac{(\text{compound})}{(\text{compound}) + K_d}$$

430

431 4.4.4.1. Calculate the FO using the independent  $K_d$  values obtained for each individual  
432 plate. Plot the results, mean, and standard deviations of the FO against the concentration of  
433 the compound.

434

435 4.4.4.2. Report the FO with values ranging from 0 to 1 or as a percentage with values  
436 ranging from 0%–100%.

437

#### 438 **REPRESENTATIVE RESULTS:**

##### 439 **Assessing the stability and concentration of type I and type III collagen immobilized in** 440 **gels/films**

441 The quantification of the collagen concentration immobilized per well was carried out using  
442 three different conditions: a) in wells without washing with PBS after immobilizing the  
443 proteins (no wash); b) in wells with a wash step (twice with PBS) after immobilization to  
444 remove any uncoated protein; c) in wells after incubation with PBS for 1 h (PBS mimic  
445 experiment). The PBS incubation mimicking step was performed to understand the stability  
446 of the collagen gel/film following incubation with a solution containing the candidate  
447 compound during the actual binding assay. Quantifying how much collagen is immobilized  
448 per well is crucial for accurately calculating and comparing the bound fraction and  
449 dissociation constant ( $K_d$ ) of a compound toward different targets, especially when those  
450 targets have different coating efficiencies. Erreur ! Source du renvoi introuvable. shows a  
451 representative stability assay for type III collagen, from which it is evident that the amount  
452 of collagen that remained immobilized on the wells decreased when washing and/or  
453 incubation steps were included. The results demonstrate that a greater loss of collagen from  
454 the gel/film occurs during the washing step and less loss occurs during the incubation step.  
455 However, washing is a crucial step during an *in vitro* binding assay to ensure that the  
456 unbound compound is removed. For this reason, it is important that the amount of collagen  
457 that remains coated within the well, and not the amount of collagen initially immobilized, is  
458 calculated and used for the normalization of the results of the *in vitro* binding assay. The  
459 optimized conditions that resulted in the reproducible immobilization of collagen and the  
460 corresponding amount of collagen that was immobilized after following the washing and  
461 incubation steps are reported in Erreur ! Source du renvoi introuvable..

462

##### 463 ***In vitro* Eu(III) TRF binding assay to characterize the binding of Eu(III)-DO3AAm-CBP** 464 **toward type I and type III collagen**

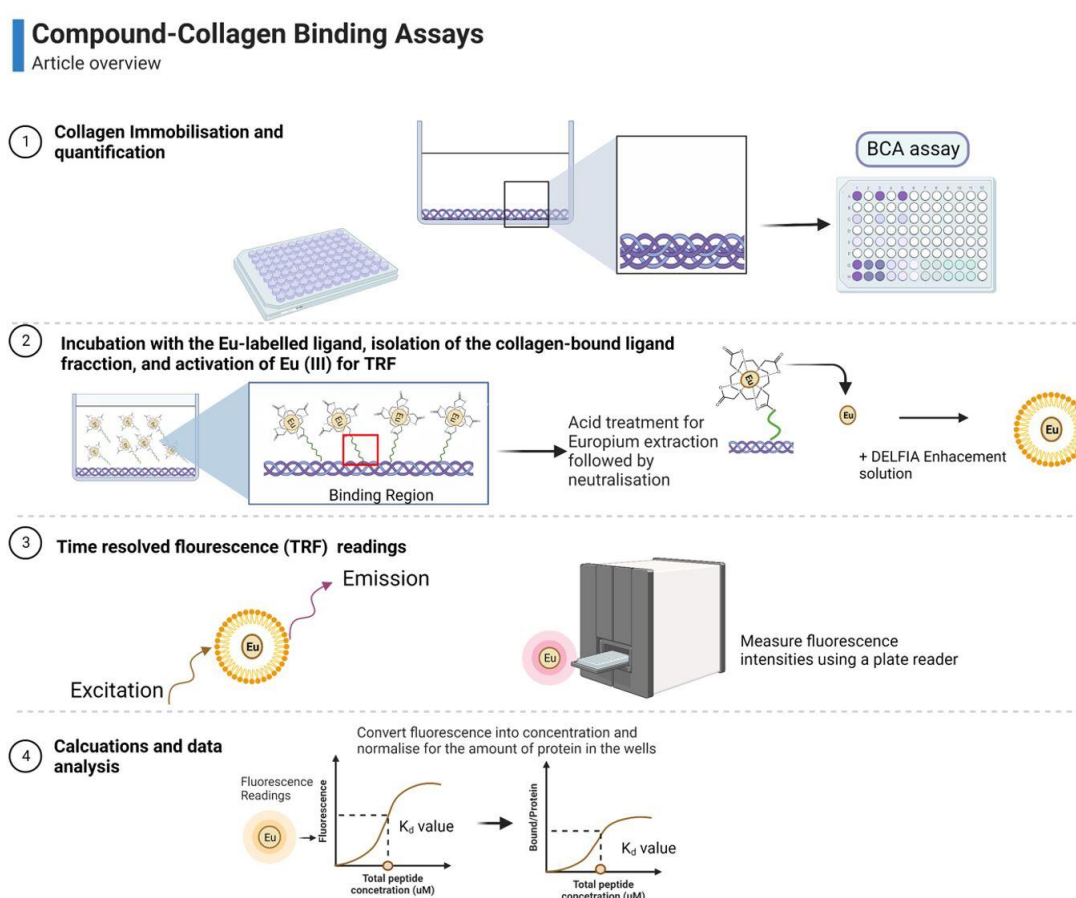
465 A representative analysis and results obtained from an *in vitro* Eu(III) TRF experiment to  
466 investigate the affinity of the Eu(III)-DO3AAm-CBP compound toward collagen type I and  
467 type III are shown in Erreur ! Source du renvoi introuvable.. The bound fluorescence  
468 readings and corresponding  $K_d$  values of the candidate collagen binding compound are  
469 shown in **Figure 8A**. The results show that the candidate compound bound non-specifically  
470 to type I collagen (as the curve does not reach saturation), and, therefore, no  $K_d$  value was  
471 reported. In contrast, the candidate compound was shown to bind to type III collagen with a  
472  $K_d$  value of  $4.2 \mu\text{M} \pm 0.7 \mu\text{M}$ . As the coating efficiencies of type I and III collagen are different  
473 (as shown in **Table 3**), a normalization step was implemented to account for the amount of

474 immobilized collagen per well. To achieve that, the standard curve obtained from the total  
 475 compound in solution (**Figure 8B**) was used to convert the bound fluorescence readings into  
 476 concentration. These values were then normalized by dividing the bound fluorescence  
 477 readings by the concentration of collagen coated onto the wells to obtain the plot shown in  
 478 **Figure 8C**, in which the bound protein data for type I and III collagen could be presented on  
 479 the same plot. It must be noted that although the  $K_d$  values were not altered by the  
 480 normalization, in this particular example, the results could be plotted and directly compared  
 481 using the same graph. The fractional occupancy results, shown in **Figure 8D**, demonstrated  
 482 that 71% of the collagen was occupied by the compound at the highest concentration of 10  
 483  $\mu\text{M}$ .

484

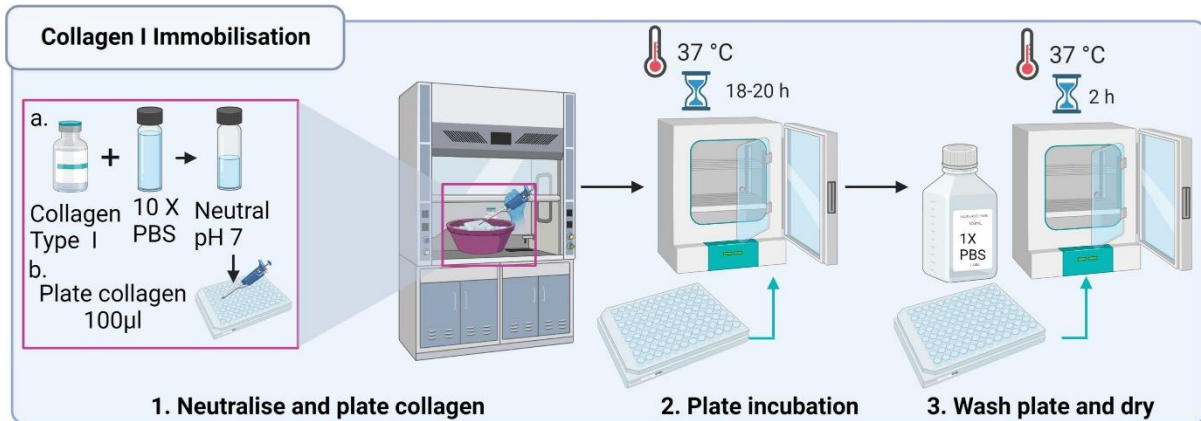
485 **FIGURE AND TABLE LEGENDS:**

486



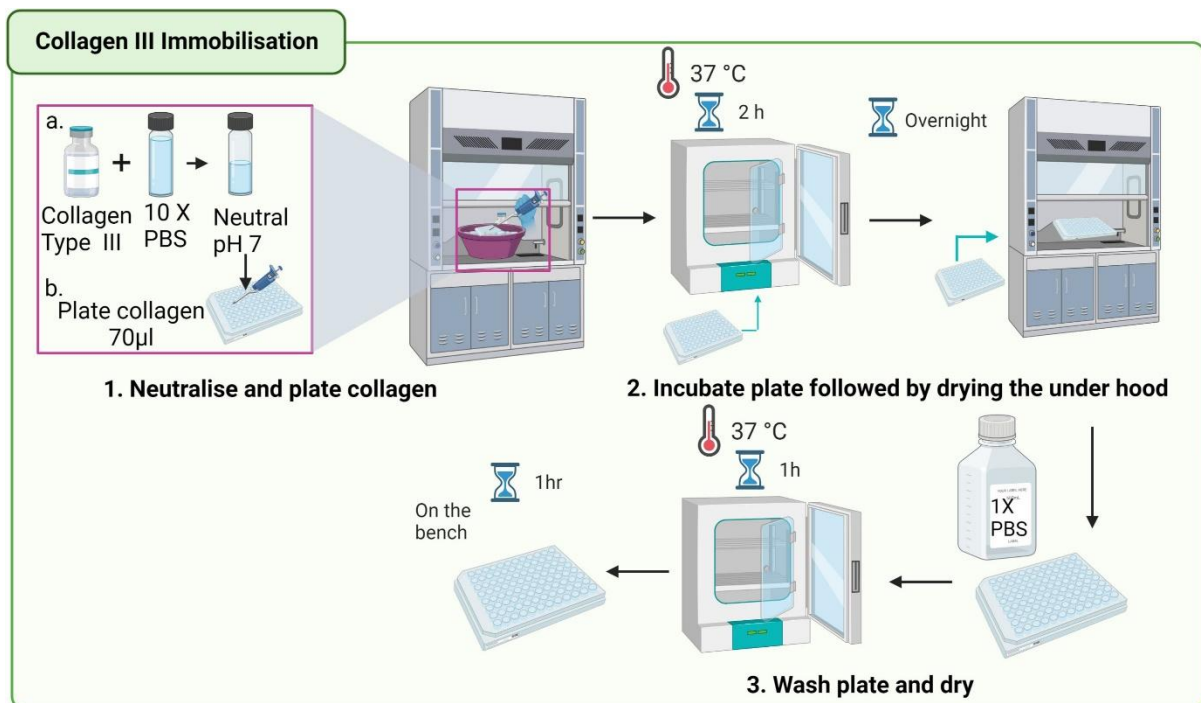
487 **Figure 1: Overview of the methodology used to study compound–protein binding**  
 488 **interactions using Eu(III) TRF.** Created with BioRender.com.

489



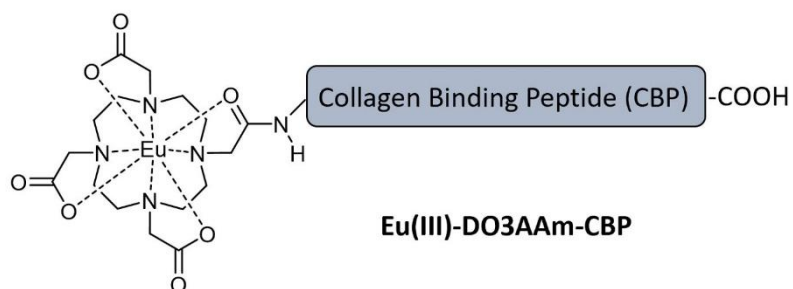
490  
491  
492  
493

**Figure 2: Workflow to immobilize type I collagen.** Created with BioRender.com.



494  
495  
496

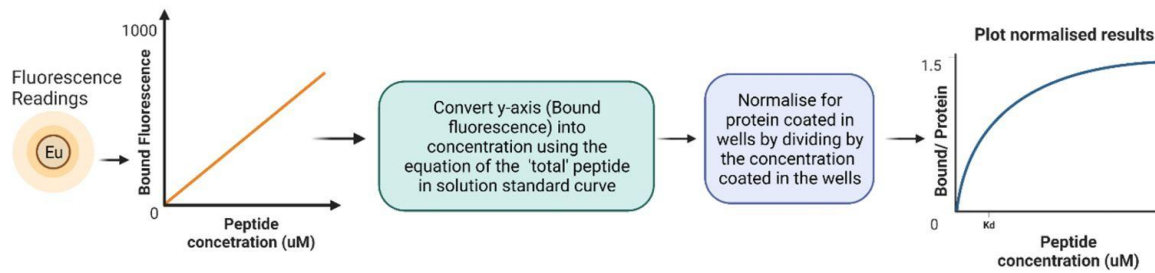
**Figure 3: Workflow to immobilize type III collagen.** Created with BioRender.com.



497  
498  
499

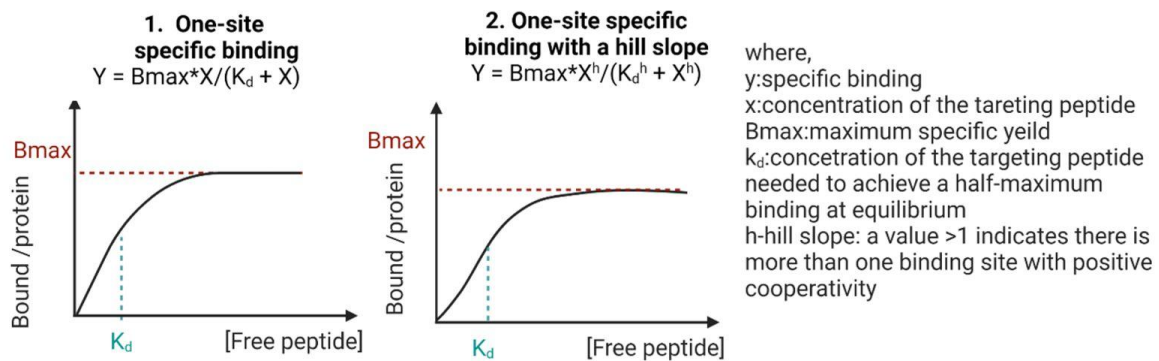
**Figure 4: Chemical structure of the Eu(III)-DOTA-monoamide derivative carrying a collagen-binding peptide (CBP) used for the *in vitro* binding studies.**

500



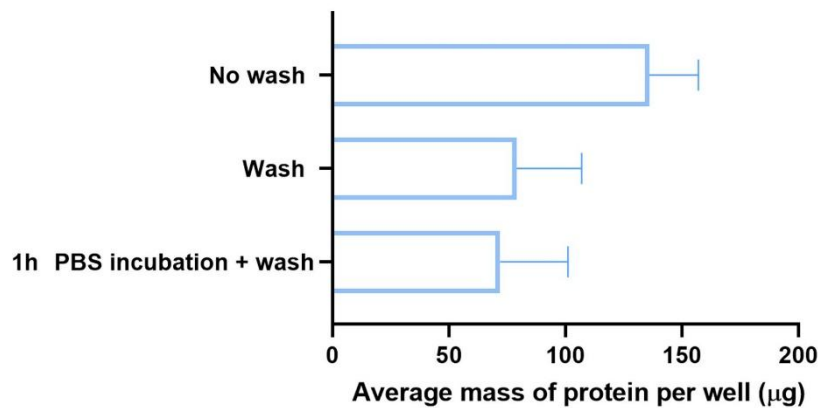
501  
502  
503  
504  
505

**Figure 5: Overview of the data analysis pipeline to calculate the dissociation constant following the *in vitro* binding assay.** Created with BioRender.com.



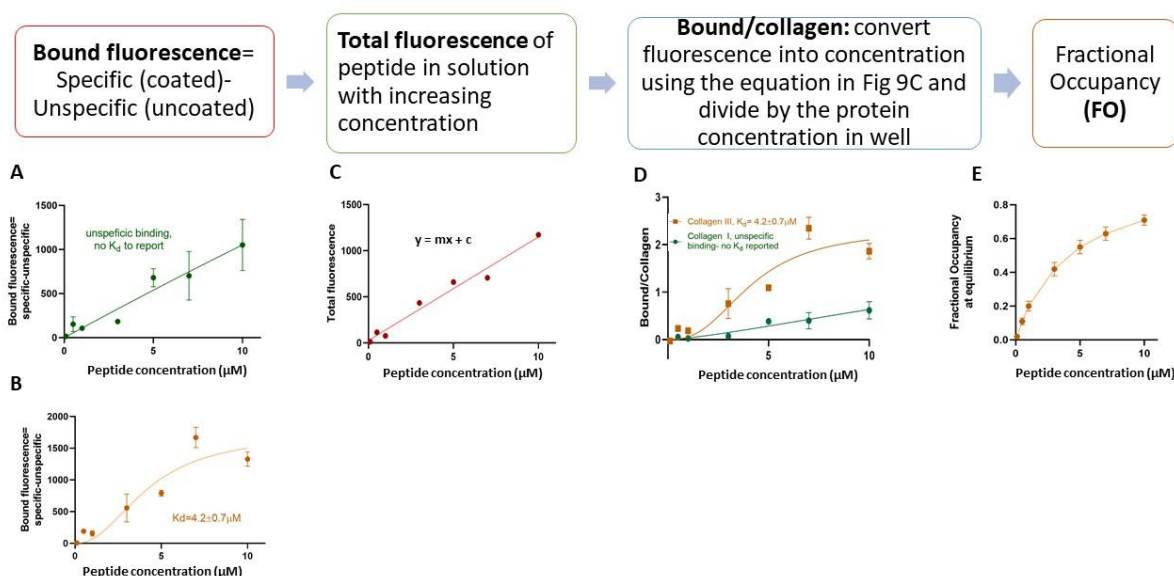
506  
507  
508  
509  
510

**Figure 6: Fitting models used in the binding assays to obtain the  $K_d$  Values.** Created with BioRender.com.



511  
512  
513  
514  
515  
516  
517  
518  
519

**Figure 7: Amount of immobilized type III collagen in three experimental conditions.** No wash = measuring the immobilized collagen directly after incubation; wash = washing the plate twice with 100  $\mu$ L of PBS; 1 h PBS mimic & wash = incubation for 1 h with PBS followed by two rounds of washes with PBS to study the stability of the film before using the microplates for further *in vitro* binding experiments (n = 4 represented as the mean from duplicate readings and two independent experiments; error bars = standard deviation)



520  
 521 **Figure 8: *In vitro* binding analysis pipeline. (A,B).** *In vitro* Eu(III) TRF binding curves using  
 522 Eu(III)-DO3AAm-CBP and immobilized type I and type III collagen, respectively. (C) Total  
 523 fluorescence readings of the Eu(III)-DO3AAm-CBP in solution. (D) Calculation of the bound  
 524 compound/protein by rearranging the equation from **Figure 8C** to convert the fluorescent  
 525 values into concentration and then dividing by the concentration of the immobilized protein  
 526 in the wells. (E) The fractional occupancy analysis of the candidate compound against type  
 527 III collagen gave an FO of 71 %. The results reported are the mean values of triplicate  
 528 readings within the same plate and from two independent plate readings (error bars =  
 529 standard deviation).

530  
 531  
 532

533 **Table 1: Summary of the main differences between the intrinsic characteristics of type I**  
 534 **and type III collagen.** Adopted from Eryilmaz et al.<sup>13</sup>.

Characteristic	Collagen Type I	Collagen Type III
Branches	Linear	Globular with branch formation likely to collapse
Polarity	Non-polar	More polar
Fibril assembly	Rapid	Slower transition from globular to extended-high nucleation rate but slow assembly
Fibrils	Straight, lateral growth	Lower propensity to nucleate straight fibrils-interconnected

535  
 536



537

538 **Table 2: Parameters for Eu(III) TRF measurements.**

Excitation Wavelength	340 nm
Emission Wavelength	619 nm
Integration Time	400 $\mu$ s
Lag Time	400 $\mu$ s

539

540

541

542 **Table 3: Optimized conditions for the immobilization of type I and type III collagen and the**  
543 **quantified amount immobilized.**

Protein	Immobilisation protocol	Coating characteristic	Volume added per well	Mass of collagen coated post-PBS mimic ( $\mu$ g)
Collagen Type I	37 ° tissue culture incubator overnight	Gel	100 $\mu$ l	240
Collagen Type III	37° for 2hrs; laminar flow under the hood overnight	Clear film	70 $\mu$ l	70

544

545

546

547

548 **Supplemental File 1: Preparation of the acidic solution (AS) and buffering solution (BS) and**  
549 **calibration of the volume.**

550

551 **DISCUSSION:**

552 This work presents a reproducible method for immobilizing type I and type III collagen. It  
553 also demonstrates a protocol for acquiring, analyzing, and interpreting *in vitro* Eu(III) TRF  
554 binding data to characterize the binding properties of a candidate ligand toward type I and  
555 III collagen. The protocols for immobilizing type I and type III collagen presented here were  
556 developed and optimized considering previously published work on type I and type III  
557 collagen fibrillogenesis *in vitro*<sup>13,16</sup>. Specifically, the reproducible coating of type I and III  
558 collagen was achieved by optimizing critical conditions, including the type of microplates,  
559 the pH, the temperature, and the ionic concentration of the buffer. Given that collagens  
560 self-assemble with increasing pH values and temperature, the neutralization and plating

561 steps for immobilizing collagen must be completed on ice and in the cold room. This ensures  
562 that the nucleation rate of collagen, the first step of fibrillogenesis, does not start before the  
563 collagen comes into contact with the well but rather occurs within the well after the  
564 temperature is increased during the incubation step. By quantifying the amount of protein  
565 in each well, it was found that type I collagen coated reproducibly and stably using non-  
566 binding specific microplates that were coated with a non-ionic hydrophilic surface. In  
567 contrast, type III collagen, showed reproducible and stable coating using tissue culture  
568 polystyrene- microplates that were exposed to plasma gas, making the microplate more  
569 hydrophilic. Immobilization protocols for type III collagen are less explored compared with  
570 those available for type I collagen, and, therefore, this protocol is unique. Although the  
571 immobilization protocols used for type I and type III collagen follow similar steps, there are  
572 crucial differences in the duration and temperature of the incubation due to the different  
573 intrinsic characteristics of the two collagen types. It is known that type III collagen has a  
574 faster nucleation rate and a slower growth rate than type I collagen, and these differences  
575 were considered when establishing this protocol (**Table 1**)<sup>13</sup>. For this reason, type III collagen  
576 requires incubation at 37 °C for only 2 h, whereas type I collagen is incubated for 18–20 h.

577  
578 The coating efficiency—how much of each collagen was coated onto the wells—was also  
579 studied, and the stability of the coating under different protocols, especially after washing  
580 and after incubating with PBS for 1 h, was investigated. The stability of the coated protein is  
581 crucial for the reproducible screening of the binding properties of a compound toward the  
582 target and the accurate calculation of the  $K_d$  and FO values. This is a step that is rarely  
583 performed, and binding protocols typically only quantify the concentration of the  
584 immobilized protein at the start of the experiment (after immobilization but prior to the  
585 incubation)<sup>16</sup>. However, because both the coating efficiency and stability of the coated  
586 protein may vary between different proteins, it is important to determine how much of the  
587 initial protein remains stably coated within the well at the end of the binding experiment  
588 and, therefore, contributes toward the final measurement. Knowing that there is a  
589 reproducible amount of protein coated on the plates is important when studying the  
590 interactions of these proteins with binding molecules, as this contributes directly to the  
591 fluorescence reading from the Eu(III)-labeled compound. Normalizing the bound  
592 fluorescence measurements with the amount of protein immobilized in the well (bound  
593 protein) does not affect the  $K_d$  or FO per se. However, such normalization leads to the  
594 rescaling of the data plotted on the y-axis of the binding curve, enabling the direct  
595 comparison of the binding profile of the same compound toward different targets with  
596 different immobilization efficiencies.

597  
598 In the analysis, it is also important to account for the non-specific binding of the compound  
599 to the experimental matrix (i.e., the plastic plate) rather than assuming that the readings  
600 acquired from the coated wells solely represent compound bound to collagen. This was  
601 accounted for by subtracting the non-specific binding of the compound to the plate  
602 (uncoated wells) from the specific reading, represented as “bound fluorescence” (collagen-  
603 coated wells), under the same TRF measurement conditions.

604  
605 Eu(III) TRF-based methods have been widely used for *in vitro* binding studies<sup>23–25</sup>. It is a  
606 flexible assay that can be used in multiple applications, such as immune assays, cell  
607 cytotoxicity studies, enzyme assays, and binding studies, as demonstrated here and in

608 previous work<sup>23,26</sup>. It is also highly sensitive and takes advantage of time-resolved  
609 fluorescence properties to eliminate any non-specific background fluorescence signals that  
610 may be observed in conventional direct readings<sup>21</sup>. In standard DELFIA applications, users  
611 are able to use the standard enhancement solution to efficiently extract Eu(III) from its  
612 complexes. However, the decomplexation of Eu(III) from Eu(III)-DO3AAm-like complexes is  
613 difficult because of the very high kinetic inertness of such complexes, which means that  
614 decomplexation will be far from being complete and reproducible. A protocol to achieve  
615 Eu(III) decomplexation from such complexes has been proposed by De Silva et al.<sup>21</sup>. Such a  
616 protocol involves the incubation of the Eu(III)-DO3AAm complex with a very acidic solution  
617 (AS, 2 M HCl) for 2 h, followed by the addition of a neutralizing solution (NS, 2 M NaOH) to  
618 bring the pH back to neutrality. The enhancement solution is then added to activate the  
619 Eu(III) and to adjust the pH to be in the optimal range (3.0–3.5) for TRF readings. However, it  
620 was found that small volume inaccuracies in the amounts of acid and neutralizing solutions  
621 added to microwells could lead to significant fluctuations in the final pH, which could affect  
622 the intensity of the Eu(III) TRF signal. Thus, the protocol was modified by adding a strong  
623 glycine buffer to the NaOH solution to obtain the buffering solution (2 M NaOH and 2 M  
624 glycine). After treatment with the acid solution to extract Eu(III), the pH is adjusted directly  
625 to 3.2 in a very consistent and reproducible manner by the addition of a calibrated amount  
626 of the buffering solution. Finally, the enhancement solution can be added for Eu(III) re-  
627 coordination and self-association into TRF active micelles.

628  
629 A limitation of the Eu(III) TRF assay is that the maximum concentration of the Eu(III)-labeled  
630 compound that can be used in the assay is 10–15  $\mu\text{M}$  because, at higher concentrations, the  
631 extraction of Eu(III) and the formation of micelles are no longer linear. Another method that  
632 has been used to measure  $K_d$  values is by using compounds labeled with other lanthanides,  
633 such as Gd(III). In this approach, the Gd(III) concentration is measured in the supernatant  
634 collected after the incubation of the Gd(III)-labeled compound with the target using ICP-MS.  
635 The ICP-MS of the supernatant collected after the incubation of the compound provides an  
636 indirect measurement of the bound fraction remaining in the well by subtracting the  
637 amount of Gd(III) in the supernatant from the “total gadolinium” concentration that was  
638 initially added in the well. Despite the indirect measurement of the “bound fraction”, this  
639 approach yields comparable binding affinities to those measured with high-performance  
640 liquid chromatography (HPLC)<sup>16</sup>. The ICP-MS method is useful in cases where the  $K_d$  may be  
641 high, meaning concentrations of the compound higher than the 10–15  $\mu\text{M}$  limit of the  
642 DELFIA assay are required in order to reach the plateau (saturation) of the binding curve  
643 and, thus, accurately calculate the  $K_d$ . Another technique to study the interactions between  
644 molecules is SPR<sup>27</sup>. This is an optical technique based on the immobilization of a target  
645 protein on a gold film and the analysis of the binding of another protein/molecule in a  
646 mobile state. The advantage of SPR is that it measures the interactions directly with no need  
647 for any fluorophore or lanthanide complexation to measure the binding response. However,  
648 the limitations of this technique include the complexity of optimizing the immobilization  
649 process (which can compromise the binding of the epitope), the difficulty of determining  
650 non-specific binding, and the cost<sup>28</sup>.

651  
652 This study presents an optimized protocol that enables the reproducible immobilization of  
653 type I and type III collagen, a detailed methodology for performing Eu(III) TRF assays to

654 study compound–collagen interactions, and a clear workflow for analyzing and interpreting  
655 the results.

656

#### 657 **ACKNOWLEDGMENTS:**

658 We are grateful to the following funders for supporting this work: (1) the UK Medical  
659 Research Council (MR/N013700/1) and King’s College London member of the MRC Doctoral  
660 Training Partnership in Biomedical Sciences; (2) BHF program grant RG/20/1/34802; (3) BHF  
661 Project grant PG/2019/34897; (4) King’s BHF Centre for Research Excellence grant  
662 RE/18/2/34213; (5) the ANID Millennium Science Initiative Program – ICN2021\_004; and (6)  
663 ANID Basal grant FB210024.

664

#### 665 **DISCLOSURES:**

666 The authors have no conflicts of interest to disclose.

667

#### 668 **REFERENCES:**

- 669 1. Distler, J. H. W. et al. Review: Frontiers of antifibrotic therapy in systemic sclerosis.  
670 *Arthritis and Rheumatology*. **69** (2), 257–267 (2017).
- 671 2. Wynn, T. A. Fibrotic disease and the TH1/TH2 paradigm. *Nature Reviews*  
672 *Immunology*. **4** (8), 583–594 (2004).
- 673 3. Saha, P. et al. Magnetic resonance T<sub>1</sub> relaxation time of venous thrombus is  
674 determined by iron processing and predicts susceptibility to lysis. *Circulation*. **128** (7), 729–  
675 736 (2013).
- 676 4. Mirshahi, M. et al. Defective thrombolysis due to collagen incorporation in fibrin  
677 clots. *Thrombosis Research*. **8**, 73–80 (1988).
- 678 5. Comerota, A. J. The ATTRACT trial: Rationale for early intervention for iliofemoral  
679 DVT. *Perspectives in Vascular Surgery and Endovascular Therapy*. **21** (4), 221–225 (2009).
- 680 6. Bateman, E. D., Turner-Warwick, M., Adelman-Grill, B. C. Immunohistochemical  
681 study of collagen types in human foetal lung and fibrotic lung disease. *Thorax*. **36** (9), 645–  
682 653 (1981).
- 683 7. Pawelec, K. M., Best, S. M., Cameron, R. E. Collagen: A network for regenerative  
684 medicine. *Journal of Materials Chemistry B*. **4** (40), 6484–6496 (2016).
- 685 8. Frantz, C., Stewart, K. M., Weaver, V. M. The extracellular matrix at a glance. *Journal*  
686 *of Cell Science*. **123** (24), 4195–4200 (2010).
- 687 9. Copes, F., Pien, N., Van Vlierberghe, S., Boccafoschi, F., Mantovani, D. Collagen-  
688 based tissue engineering strategies for vascular medicine. *Frontiers in Bioengineering and*  
689 *Biotechnology*. **7**, 166 (2019).
- 690 10. Veis, A. The biochemistry of collagen. *Annals of Clinical and Laboratory Science*. **5** (2),  
691 123–131 (1975).
- 692 11. Bielajew, B. K., Hu, J. C., Athanasiou, K. A. Collagen: Quantification, biomechanics,  
693 and role of minor subtypes in cartilage. *Nature Reviews Materials*. **5**, 730–747 (2020).
- 694 12. Zhao, Z. et al. Structural and functional plasticity of collagen fibrils. *DNA and Cell*  
695 *Biology*. **38** (4), 367–373 (2019).
- 696 13. Eryilmaz, E., Teizer, W., Hwang, W. In vitro analysis of the co-assembly of type-I and  
697 type-III collagen. *Cellular and Molecular Bioengineering*. **10** (1), 41–53 (2017).
- 698 14. Jagnow, J., Clegg, S. *Klebsiella pneumoniae* MrkD-mediated biofilm formation on  
699 extracellular matrix- and collagen-coated surfaces. *Microbiology*. **149** (9), 2397–2405 (2003).
- 700 15. O’Sullivan, D., O’Neill, L., Bourke, P. Direct plasma deposition of collagen on 96-well

- 701 polystyrene plates for cell culture. *ACS Omega*. **5** (39), 25069–25076 (2020).
- 702 16. Caravan, P. et al. Collagen-targeted MRI contrast agent for molecular imaging of  
703 fibrosis. *Angewandte Chemie - International Edition*. **46** (43), 8171–8173 (2007).
- 704 17. Copeland, R. A. *Enzymes: A Practical Introduction to Structure, Mechanism, and Data*  
705 *Analysis*. John Wiley & Sons, Ltd. Hoboken, NJ (2000).
- 706 18. Salahudeen, M. S., Nishtala, P. S. An overview of pharmacodynamic modelling,  
707 ligand-binding approach and its application in clinical practice. *Saudi Pharmaceutical*  
708 *Journal*. **25** (2), 165–175 (2017).
- 709 19. Bünzli, J. C. G., Piguet, C. Taking advantage of luminescent lanthanide ions. *Chemical*  
710 *Society Reviews*. **34** (12), 1048–1077 (2005).
- 711 20. Hemmilii, I. Luminescent lanthanide chelates - A way to more sensitive diagnostic  
712 methods. **225** (1–2), 480–485 (1995).
- 713 21. De Silva, C. R., Vagner, J., Lynch, R., Gillies, R. J., Hruby, V. J. Optimization of time-  
714 resolved fluorescence assay for detection of europium-tetraazacyclododecyltetraacetic acid-  
715 labeled ligand-receptor interactions. *Analytical Biochemistry*. **398** (1), 15–23 (2010).
- 716 22. Digilio, G., Lacerda, S., Lavin Plaza, B., Phinikaridou, A. Extracellular matrix targeted  
717 MRI probes. *Analysis & Sensing*. **3** (1), e202200039 (2022).
- 718 23. Phinikaridou, A. et al. Tropoelastin: A novel marker for plaque progression and  
719 instability. *Circulation. Cardiovascular imaging*. **11** (8), e007303 (2018).
- 720 24. Guzaeva, T. V. et al. Protein A used in DELFIA for the determination of specific  
721 antibodies. *Immunology Letters*. **35** (3), 285–289 (1993).
- 722 25. Nasiri, A. H., Nasiri, H. R. Polymerase assays for lead discovery: An overall review of  
723 methodologies and approaches. *Analytical Biochemistry*. **563**, 40–50 (2018).
- 724 26. Capuana, F. et al. Imaging of dysfunctional elastogenesis in atherosclerosis using an  
725 improved gadolinium-based tetrameric MRI probe targeted to tropoelastin. *Journal of*  
726 *Medicinal Chemistry*. **64** (20), 15250–15261 (2021).
- 727 27. Drescher, D. G., Drescher, M. J., Ramakrishnan, N. A. Surface plasmon resonance  
728 (SPR) analysis of binding interactions of proteins in inner-ear sensory epithelia. *Methods in*  
729 *Molecular Biology*. **493**, 323–343 (2009).
- 730 28. Murali, S., Rustandi, R. R., Zheng, X., Payne, A., Shang, L. Applications of surface  
731 plasmon resonance and biolayer interferometry for virus–ligand binding. *Viruses*. **14** (4), 717  
732 (2022).